

Acanthamoeba spp. monoclonal antibody against a CPA2 transporter: a promising molecular tool for acanthamoebiasis diagnosis and encystment study

Research Article

*Those authors contributed equally for the manuscript

Cite this article: Weber-Lima MM, Prado-Costa B, Becker-Finco A, Costa AO, Billilad P, Furst C, de Moura JF, Alvarenga LM (2020). *Acanthamoeba* spp. monoclonal antibody against a CPA2 transporter: a promising molecular tool for acanthamoebiasis diagnosis and encystment study. *Parasitology* **147**, 1678–1688. <https://doi.org/10.1017/S0031182020001778>


Received: 11 July 2020
Revised: 3 September 2020
Accepted: 6 September 2020
First published online: 21 September 2020

Key words:

Acanthamoeba; CPA2 transporters; diagnosis; encystment; flow cytometry; monoclonal antibody

Author for correspondence:

Larissa Magalhães Alvarenga,
E-mail: lmalvarenga@ufpr.br;
lmalvarenga@gmail.com

Michele Martha Weber-Lima^{1,*}, Bianca Prado-Costa^{1,*}, Alessandra Becker-Finco¹, Adriana Oliveira Costa², Philippe Billilad³, Cinthia Furst⁴, Juliana Ferreira de Moura¹ and Larissa Magalhães Alvarenga¹ 

¹Laboratório de Imunoquímica, Departamento de Patologia Básica, Universidade Federal do Paraná, Curitiba-PR, Brazil; ²Departamento de Análises Clínicas e Toxicológicas, Faculdade de Farmácia, Universidade Federal de Minas Gerais, Belo Horizonte-MG, Brazil; ³IPSIT, School of Pharmacy, University Paris-Saclay, Châtenay-Malabry, France and ⁴Departamento de Patologia, Centro de Ciências da Saúde, Universidade Federal do Espírito Santo, Vitória, ES, Brazil

Abstract

Free-living amoeba of the genus *Acanthamoeba* are ubiquitous protozoa involved in opportunistic and non-opportunistic infection in humans, such as granulomatous amoebic encephalitis and amoebic keratitis. Both infections have challenging characteristics such as the formation of the resistant cysts in infected tissues, hampering the treatment and most usual diagnosis depending on time-consuming and/or low sensitivity techniques. The use of monoclonal antibodies presents itself as an opportunity for the development of more effective alternative diagnostic methods, as well as an important and useful tool in the search for new therapeutic targets. This study investigated the possibility of using a previously produced monoclonal antibody (mAb3), as a diagnostic tool for the detection of *Acanthamoeba* trophozoites by direct and indirect flow cytometry and immunofluorescence. Immunoprecipitation assay and mass spectrometry allowed the isolation of the antibody's target and suggested it is a transporter part of the CPA (cation: proton antiporter) superfamily. *In vitro* tests indicate an important role of this target in *Acanthamoeba*'s encystment physiology. Our results support the importance of studying the role of CPA2 transporters in the context of acanthamoebiasis, as this may be a way to identify new therapeutic candidates.

Introduction

Acanthamoeba is a genus of free-living protozoa found in several environments, living as trophozoites (the vegetative stage) or cysts (the dormant, resistant stage) (Visvesvara *et al.*, 2007). Despite being free-living organisms, these amoebae may sometimes act as opportunistic pathogens causing serious diseases (Marciano-Cabral and Cabral, 2003).

One of the forms of human acanthamebiasis is the granulomatous amoebic encephalitis (GAE), an infection that usually occurs in immunocompromised individuals and evolves from skin lesions or previous lung involvement (Marciano-Cabral and Cabral, 2003). GAE is considered a rare infection of the central nervous system, but the real incidence is unknown due to underdiagnosis (Duggal *et al.*, 2017). The high current lethality of GAE (about 90%) indicates that better approaches to diagnosis and treatment are urgently needed (Kalra *et al.*, 2020).

Acanthamoeba is also involved in a severe corneal infection that affects mainly contact lens wearers, the *Acanthamoeba* keratitis (AK). AK is characterized by pain, redness, tearing and photophobia, which occurs as consequences of corneal lesions that can progress to visual impairment and even blindness, if not properly treated (Trabelsi *et al.*, 2012; Lorenzo-Morales *et al.*, 2013). The incidence of AK has increased in recent decades as a result of the increasing number of contact lens wearers, with lens misuse representing the main risk factor for the infection (Trabelsi *et al.*, 2012; Lorenzo-Morales *et al.*, 2015). Consequently, AK has been perceived as an emerging disease worldwide (Carnt *et al.*, 2018; Bunsuwansakul *et al.*, 2019).

As well as for GAE, the correct diagnosis of AK is also a challenge. Clinical signs are very similar to other microbial keratitis caused by herpes virus and fungi, which can delay the specific treatment (Lorenzo-Morales *et al.*, 2015; Szentmáry *et al.*, 2019). Besides, the main laboratory diagnostic methods remain low sensitivity techniques such as the identification of *Acanthamoeba* in corneal scraping or biopsy by microscopic direct visualization or after culture, this later being considered the gold standard (Trabelsi *et al.*, 2012; Lorenzo-Morales *et al.*, 2015).

Detection of *Acanthamoeba* by immunoassays using specific antibodies can be a promising strategy to facilitate and support AK diagnosis (Khan *et al.*, 2000; Turner *et al.*, 2005). In addition to this, monoclonal antibodies are an important tool in the study of protein expression and function, improving the understanding of these organisms and helping in the search for therapeutic targets (Turner *et al.*, 2005; Fiori *et al.*, 2006; Kang *et al.*, 2018). However, the identification of

Table 1. Origin, genotype and morphological group of *Acanthamoeba* strains

Strain	Origin/Axenization	Genotype	Morphological group	Reference
AP2	Corneal scraping, Houston, TX, EUA/1973	T4	Group II	ATCC 30461
ALX	Corneal scraping, Vitória-ES, Brazil/2006	T4	Group II	Duarte <i>et al.</i> (2013)
LG	Corneal scraping, Vitória-ES, Brazil/2011	T4	Group II	Duarte <i>et al.</i> (2013)
R2P5	Domestic dust, Vitória-ES, Brazil/2011	T1	Group II	Possamai <i>et al.</i> (2018)
AR14	Domestic dust, Vitória-ES, Brazil/2007	T4	Group II	Duarte <i>et al.</i> (2013)
AR15	Domestic dust, Vitória-ES, Brazil/2007	T11	Group II	Duarte <i>et al.</i> (2013)
AC-G1	Soil, Vitória-ES, Brazil/2016	N.D.	Group I	–

N.D., not determined.

new relevant targets in the context of *Acanthamoeba* physiology is also necessary for a better comprehension of pathogenesis, which is yet not completely understood (Neelam and Niederkorn, 2017; Kalra *et al.*, 2020).

Becker-Finco *et al.* (2013) previously produced the monoclonal antibody mAb3, which can recognize only pathogenic *Acanthamoeba* isolates by enzyme-linked immunosorbent assay (ELISA), Western Blotting (WB) and indirect immunofluorescence. The present study aimed to evaluate mAb3's capacity of directly detecting *Acanthamoeba* trophozoites by flow cytometry and immunofluorescence conjugating it to a fluorophore. In addition, mAb3's target protein was investigated concerning its possible involvement in the encystation kinetics taking into consideration mAb3's influence in this process.

Materials and methods

Acanthamoeba strains

Seven strains were used in this study, three of them being clinical samples isolated from corneal scrapings of AK patients (AP2, ALX and LG) and four obtained from environmental sources, isolated from domestic dust (AR14, AR15, R2P5) and soil (AC-G1) (Table 1). Genotypes and morphological groups of the strains were previously determined as outlined in Table 1. *Acanthamoeba* cultures were maintained axenically in peptone, yeast extract and glucose medium – PYG (20 g L⁻¹ proteose peptone, 1 g L⁻¹ yeast extract, 0.1 mol L⁻¹ glucose, 4 mol L⁻¹ MgSO₄, 0.4 mmol L⁻¹ CaCl₂, 3.4 mmol L⁻¹ sodium citrate, 0.05 mmol L⁻¹ Fe(NH₄)₂(SO₄)₂ and 2.5 mmol L⁻¹ of both Na₂HPO₄ and KH₂PO₄) pH 6.5, at 28 °C, supplemented with 10% fetal bovine serum (FBS) and 1% pen/strep (solution containing 10⁴ units mL⁻¹ of penicillin and 10⁴ µg mL⁻¹ of streptomycin, Gibco).

Monoclonal antibody (mAb3) production and purification

Hybridoma cells secreting mAb3 (Becker-Finco *et al.*, 2013) were cultured in Dulbecco's modified Eagle's medium (DMEM) supplemented with 10% FBS and 1% pen/strep (solution containing 10⁴ units mL⁻¹ of penicillin and 10⁴ µg mL⁻¹ of streptomycin, Gibco). Cells were maintained at 37 °C, in a humidified atmosphere with 5% CO₂. Cell supernatant was collected and mAb3 (IgG) purification was carried out by immunoaffinity chromatography using protein G immobilized Sepharose column. Protein concentration of samples was determined by Bradford reagent (Bio-Rad Laboratories, USA).

FITC conjugation of antibodies

The conjugation protocol of mAb3 and a nonspecific mouse IgG (LimAb7, an antibody against *Loxosceles intermedia* venom,

Karim-Silva *et al.*, 2016) to fluorescein isothiocyanate (FITC) was adapted from the manufacturer's instructions (Sigma-Aldrich, Inc). Antibodies were dialysed against carbonate buffer 0.1 M pH 9, the protein concentration was adjusted to 1 mg mL⁻¹ and samples were mixed with FITC diluted in dimethyl sulfoxide (DMSO) (1 mg mL⁻¹), under the following conditions: for each 1 mL of antibody solution, 50 µL of FITC solution was added very slowly under gentle stirring. The mix was incubated in the dark for 8 h at 4 °C, followed by addition of NH₄Cl (50 mmol L⁻¹), and after another 2 h, the addition of glycerol 5%. Unbound FITC was removed by gel filtration with Sephadex G25M resin. Finally, to determine the protein concentration of antibody conjugates, the absorbance of samples was measured by spectrophotometry at 280 and 495 nm wavelengths applying the formula: [IgG] (mg mL⁻¹) = [A280 - (0.35 × A495)]/1.4.

Gene sequencing of mAb3 light and heavy chain variable regions

Total RNA of mAb3 secreting hybridomas was isolated using TRIzol reagent, followed by amplification of the cDNA encoding the antibody's light (VL) and heavy (VH) variable chain sequences, by RT-PCR (reverse transcription polymerase chain reaction). Herein, the primers used for RT-PCR were VhRevU/VhForU for the heavy variable chain (VH), VkForU and VkRev1-9 for hypothetical kappa chain and V1RevU/V1ForU for hypothetical lambda chain as previously reported (Fields *et al.*, 2013). Confirmation of DNA fragment amplification was done by agarose (1.5%) gel electrophoresis. These fragments were purified and cloned into the PGEM T-easy vector, using T4 ligase. Competent *Escherichia coli* TG1 cells with the plasmids that contained the desired insert were selected, purified plasmid DNA was extracted through miniprep method, DNA concentration was measured by spectrophotometry (Thermo Scientific NanoDrop 2000) and fragment analysis was done by agarose (1.5%) gel electrophoresis. DNA purification and sequencing reaction used T7 universal primer (TAA TAC GAC TCA CTA TAG GG), performed by the 3500XL sequencer, Applied Biosystems, Genetic Analyser, following the DNA sequencing model by SANGER. Sequencing reaction times were adapted according to the protocol described by Fields *et al.* (2013).

Protein modelling

Antibody frameworks and complementarity-determining regions (CDRs) were identified using the international ImMunoGeneTics information system (IMGT) facilities (PMID:19900967). A three-dimensional model of the variable portion of the light and heavy chains of mAb3 was predicted through homology modelling, using the ModWeb online server. The generated models were analysed through MolProbity web service (Zhao *et al.*, 2012) and

optimization was performed through UCFC Chimera software 1.13.1 (Pettersen *et al.*, 2004).

Antigen extract preparation

To obtain protein extracts, trophozoites washed three times with Page's Saline Solution (1 mmol L⁻¹ Na₂HPO₄, 1 mmol L⁻¹ KH₂PO₄, 0.016 mmol L⁻¹ MgSO₄, 0.03 mmol L⁻¹ CaCl₂ and 2 mmol L⁻¹ NaCl) (400 × g, 5 min) were incubated for 1 h at 4 °C in lysis buffer (10 mmol L⁻¹ Tris-HCl, pH 7.6, 50 mmol L⁻¹ NaCl, 50 mmol L⁻¹ NaF, 1% Triton X-100 and Halt™ Protease Inhibitor Cocktail, Thermo Scientific) (Muinao *et al.*, 2018). The suspension was centrifuged at 3000 × g for 20 min and the protein concentration of the soluble fraction was determined by Bradford assay, taking into account proper dilution of the sample to avoid interference from any of the lysis buffer components.

Sonication for protein extraction was also performed with *Acanthamoeba* trophozoites (1 × 10⁶) and *Fusarium* sp., *Aspergillus* sp. and *Candida* sp. samples, which were used to check antibody specificity. Fungi strains were provided by TAXonline (Rede Paranaense de Coleções Biológicas) and grown in Sabouraud agar medium under controlled conditions for 7 days (28 °C, 70% humidity and a 12-h photoperiod). Fungal colonies were then transferred to a tube containing a saline solution (NaCl 145 mmol L⁻¹). *Acanthamoeba* and fungi samples were centrifuged, respectively at 1000 × g and 9000 × g, for 10 min, resulting pellets were washed and resuspended in 1 mL of PBS (phosphate-buffered saline) and 10 μL of protease inhibitor (Halt™ Protease Inhibitor Cocktail, Thermo Scientific). This suspension was sonicated at 4 °C, using 15 pulses of 1 min (40 V) with intervals of 30 s. The solution was centrifuged at 1000 × g for 10 min and protein concentration of the soluble extract was determined by Bradford assay.

ELISA

Acanthamoeba trophozoites antigens (10 μg mL⁻¹) were incubated with carbonate buffer (NaHCO₃ 100 mmol L⁻¹, pH 9.6) for 12–16 h at 4 °C in 96-well plates. The wells were then saturated in blocking solution (2% casein diluted in PBS) for 1 h at 37 °C. After that, antigens were incubated with a solution containing the mAb3 antibody in different concentrations (0.08–5.0 μg mL⁻¹), nonspecific IgG (LimAb7) or polyclonal antibodies against *Acanthamoeba* (5.0 μg mL⁻¹), diluted in incubation buffer (PBS, 0.25% casein, 0.05% tween 20), for 1 h at 37 °C. Followed by the addition of a horseradish peroxidase (HRP)-conjugated anti-mouse IgG (Sigma), diluted in incubation buffer 1:4000. Between each of the incubation steps, the wells were washed three times in washing solution (0.05% Tween-saline). Finally, specific antibody interactions were revealed with orthophenylenediamine solution (OPD), after 15 min the reaction was stopped with the addition of 20 μL of sulfuric acid (1:20). Absorbance was read in 490 nm wavelength.

Western blotting

Protein antigens from *Acanthamoeba* strains and fungi samples (1.5 or 5 μg) were separated by SDS-PAGE (sodium dodecyl sulphate–polyacrylamide gel electrophoresis) (12.5% polyacrylamide) according to the methodology described by Laemmli (1970). Migration occurred in the migration buffer (0.025 mol L⁻¹ Tris, 0.2 mol L⁻¹ glycine and 0.5% SDS, pH 8.3) under 100 V for 180 min. After SDS-PAGE migration, proteins were electro-transferred to a 0.22 μm polyvinylidene difluoride (PVDF) (Immobilon™ Transfer Membranes) or 0.45 mm nitrocellulose membrane and subjected to a 24 V current for 16 h and then to a 48 V current for another hour in transfer buffer pH 8.3

(0.2 mol L⁻¹ glycine, 0.025 mol L⁻¹ Tris and 20% (v/v) methanol). The protein electrotransfer was confirmed by Ponceau reversible staining (0.2% Ponceau solution and 10% acetic acid). The membranes were blocked with phosphate-buffered saline (PBS) containing 0.3% (v/v) Tween 20 (PBS-T 0.3%) and 3–5% (w/v) non-fat dry milk, for 1 h at 37 °C under agitation, followed by incubation at 37 °C for 2 h with the monoclonal antibody mAb3 (0.5–5.0 μg mL⁻¹). Between each incubation step, the membrane was washed three times in PBS-T 0.05% (v/v) for 5 min. After that, the membranes were incubated for 1 h at 37 °C under agitation, in the presence of peroxidase-conjugated anti-mouse IgG (Sigma), diluted 1:4000 or 1: 10 000 in PBS-T 0.05% (v/v). Binding of antibodies to the membranes was revealed by chemiluminescence and photographic film or by addition of PBS solution containing 0.025% 4-chlorine 1-naphthol diluted in 1 mL of methanol, 0.05% diaminobenzidine (DAB) and 0.04% H₂O₂ (v/v).

Tunicamycin treatment

To determine whether mAb3's target is influenced by N-glycosylation, the N-glycosylation inhibitor tunicamycin was added to *Acanthamoeba* cultures. Trophozoites were cultured in PYG medium with tunicamycin (10 μg mL⁻¹) for 72 h. Subsequently, 1 × 10⁶ *Acanthamoeba* trophozoites were analysed by indirect flow cytometry, under treatment conditions or not, against 125 μg mL⁻¹ of mAb3 and Alexa Fluor 488 goat anti-mouse IgG [H + L] conjugate Antibody (Molecular probes®) (1:300).

Immunoprecipitation and purification of the mAb3 target protein

The antibody mAb3 was incubated in a column with immobilized protein A and G Sepharose (Protein A and G Sepharose 4 Fast Flow – GE Healthcare) (1 mg mAb3 per 200 μL of protein A and 200 μL of protein G sepharose), for 1 h at room temperature under constant agitation. Sequential washes were performed with PBS pH 7.4 and pH 8.0 (two washes) followed by centrifugation at 28.500 × g for 6 min. Dimethylpimelimidate (DMP) 13 mg mL⁻¹ was added to establish a stable link (crosslinking) between the mAb3 antibody and recombinant A and G proteins, dissolved in 0.2 mol L⁻¹ triethanolamine pH 8.2 (1:1) with volume resin (VR) which was incubated for 30 min under agitation. Ethanolamine 0.1 M pH 8.2, was added (1:1) with the VR, for 5 min and centrifuged. Two washes and centrifugation steps were performed, one with ethanolamine and one with PBS pH 7.4. And 0.1 M glycine pH 2.7 was incubated twice for 5 min followed by new centrifugation. Finally, the pH was restored with PBS pH 7.4 and the column stored in PBS-0.05% sodium azide at 4 °C. All incubation steps were performed at room temperature, while centrifugations were performed at 4 °C. To purify mAb3's target protein, *Acanthamoeba* spp. sonicated extract was incubated for 24 h with the previously prepared affinity column. After 10 washes with PBS pH 7.4, the protein was eluted with 0.1 mol L⁻¹ glycine pH 2.7, protein concentrations of all eluted fractions were tested by Bradford assay and the selected fractions were separated and dialysed in PBS pH 7.4. The procedure for immunoprecipitation and purification of the mAb3 target protein was adapted from the Abcam® Crosslinking Protocol – Procedure for crosslinking the antibody to beads.

Analysis by mass spectrometry (MS) and amino acid sequence alignments

The purified mAb3 target protein was resolved by SDS-PAGE (12.5% polyacrylamide gel), stained with silver and the resulting

bands were excised and analysed by MS Platform-PR, Carlos Chagas Institute – Fiocruz. Half of the mass sample eluted from the gel was injected into the Thermo Easy-nLC 1000 chromatograph. The peptides were separated using a 60 min linear gradient of 5–40% acetonitrile, 5% DMSO, 0.1% formic acid in a 15 cm analytical column, with an internal diameter of 75 μm and C18 particles of 3 μm , heated to 60 °C. The peptides were ionized by nano electro spray (voltage of 2.7 kV) and injected in the LTQ Orbitrap XL ETD mass spectrometer (Thermo Scientific). The method of analysis was as follows: initial scan on the Orbitrap with a resolution of 15 000, followed by the selection of the 10 most intense ions, which were fragmented by collision-induced dissociation (CID) and analysed on the ion trap. Parallel to MS², a full scan was performed at Orbitrap with a resolution of 60 000. In selecting the ions, a 90-s exclusion list was used. The lock mass option was used to obtain better accuracy – error below 0.5 p.p.m. – mass of the triptych precursor peptides detected by MS. The resulting data were processed using PEAKS software. Employing *de novo* peptide sequencing, the most abundant peptides were identified and searched against *Acanthamoeba* protein databases through a basic local alignment search tool (BLASTP).

Protein sequences were obtained from the UniProt database. Sequence alignments and per cent identity analyses were performed using EMBL-EBI's Clustal Omega.

Flow cytometry

For *Acanthamoeba* detection by indirect flow cytometry (IFC), 1×10^6 trophozoites of each isolate were fixed with paraformaldehyde 4% for 20 min, blocked with albumin 1% for 1 h, incubated with mAb3 (125 $\mu\text{g mL}^{-1}$) for 12 h at 4 °C and then mixed with Goat anti-Mouse IgG (H + L), Alexa Fluor 488 conjugate Antibody (Molecular probes®) (1:300) for 1 h, in between each step, cells were washed three times with PBS. Trophozoites treated only with the anti-mouse IgG conjugate (to verify non-specific binding), and with no antibodies were used as negative controls. Fluorescence of the samples was measured by BD FACSCalibur™ flow cytometer, using the FL1-H filter (488 nm).

For direct flow cytometry (DFC), trophozoites of different strains were harvested, fixed with paraformaldehyde 2% for 30 min and blocked with albumin 1% for 1 h, between each step, cells were carefully washed in PBS once. Then, for each isolate, in duplicates, 3×10^4 trophozoites were counted using the Neubauer counting chamber and incubated with FITC-conjugated mAb3 (mAb3-FITC) (20 $\mu\text{g mL}^{-1}$) for 90 min at 37 °C (except for isolate AC-G1, which would burst under these conditions, so the incubation was done at room temperature). After that, trophozoites were centrifuged, resuspended in 400 μL of PBS and transferred to flow cytometry tubes for analysis. As negative controls, instead of the mAb3-FITC incubation step, trophozoites were either incubated with no antibodies to determine their autofluorescence or with FITC-conjugated nonspecific IgG (20 $\mu\text{g mL}^{-1}$). The fluorescence intensity of all samples was measured by BD FACSCelesta™ flow cytometer, using the 530-30 filter.

For both indirect and direct detection protocols, different concentrations of mAb3 were tested before settling for the one which yielded the best results. All flow cytometry data were analysed using Flowing Software.

Direct immunofluorescence

A portion (200–300 μL) of the same samples prepared for direct flow cytometry (DFC) analysis, was concentrated by centrifugation at 2700 $\times g$ for 5 min and resuspended in PBS (20 μL) mixed with Fluoromount™ (2 μL). After that, 10 μL of the cell suspension was pipetted on glass slides in duplicates and covered

with coverslips. The slides were observed under confocal fluorescence microscopy (Nikon A1R MP, NIKON Instruments Inc., Japan) and the resulting images were analysed using Fiji software.

Encystation assays

To evaluate the influence of mAb3 in *Acanthamoeba* encystment, the reference strain AP2 (ATCC 30461) was used. Initially, the kinetics of encystment was determined by inducing trophozoites to encyst *in vitro* using a protocol adapted from Da Rocha-Azevedo and Costa e Silva-Filho (2007). Briefly, trophozoites were harvested from cultures, washed twice in Page's saline (400 $\times g$, 5 min) to remove PYG medium and resuspended in Neff's encystation saline (NES) (95 mmol L⁻¹ NaCl, 5 mmol L⁻¹ KCl, 8 mmol L⁻¹ MgSO₄, 0.4 mmol L⁻¹ CaCl₂, 1 mmol L⁻¹ NaHCO₃ and 20 mmol L⁻¹ Tris-HCl, pH 9.0). Trophozoites were then distributed in 24-well culture plates (2.5×10^4 trophozoites in 1 mL of NES per well). At regular time intervals, the cells were observed under inverted light microscopy and at least 170 cells in 3 random microscope fields per well were analysed. The percentage of trophozoites, precysts and mature cyst was recorded. The main criteria to categorize the trophozoites was the presence of acanthopodia, while mature cysts were identified by the double cell wall. Smooth spherical cells with a single wall were classified as pre-cysts (Lorenzo-Morales *et al.*, 2008; Chávez-Munguía *et al.*, 2013).

To evaluate the effect of mAb3 on the encystation process, mAb3 diluted in PBS was added to the encystation medium in the wells at a final concentration of 1, 5, 10 and 30 $\mu\text{g mL}^{-1}$. As negative controls, trophozoites in NES were treated with PBS and with nonspecific antibodies at 1, 5, 10 and 30 $\mu\text{g mL}^{-1}$. Wells were observed after 4, 8, 12 and 24 h and the percentage of different stages of encystation was determined as described above. Precyst formation rate between observation times t_1 and t_2 was also determined as follows, based on principles discussed by Olli *et al.* (2004): (% trophozoites in t_1 – % trophozoites in t_2).

Statistical analysis

All statistical analyses were performed using GraphPad Prism 8.0.1, using two-way ANOVA, with Tukey's *post hoc* test. $P < 0.05$ was considered statistically significant.

Results

mAb3's variable sequences were confirmed as a functional murine immunoglobulin

Antibody-secreting hybridomas specific against *Acanthamoeba* antigens were produced by Becker-Finco *et al.* (2013), including mAb3. The cells of interest were defrosted and remained secreting reactive antibodies when cultivated in optimal conditions. Before functional characterization of mAb3, the RNA was extracted from the hybridomas and the regions of interest were sequenced to confirm that the molecule under study corresponds to a functional murine immunoglobulin sequence. Figure 1A shows single bands of around 350 bp, analysed by electrophoresis, of the RT-PCR products that encode the VH and V λ regions. No amplicon was observed when using sets of kappa chain-specific primers, indicating that the hybridoma transcript does not produce any functional kappa chain transcripts. Sequencing and *in silico* analyses indicated that mAb3 IGH-V and IGL-V sequences were unique. Complementary determining regions (CDRs) framework was identified using the IMGT tools. No key conserved residues were mutated in the framework regions, suggesting that the sequences were correctly rearranged and

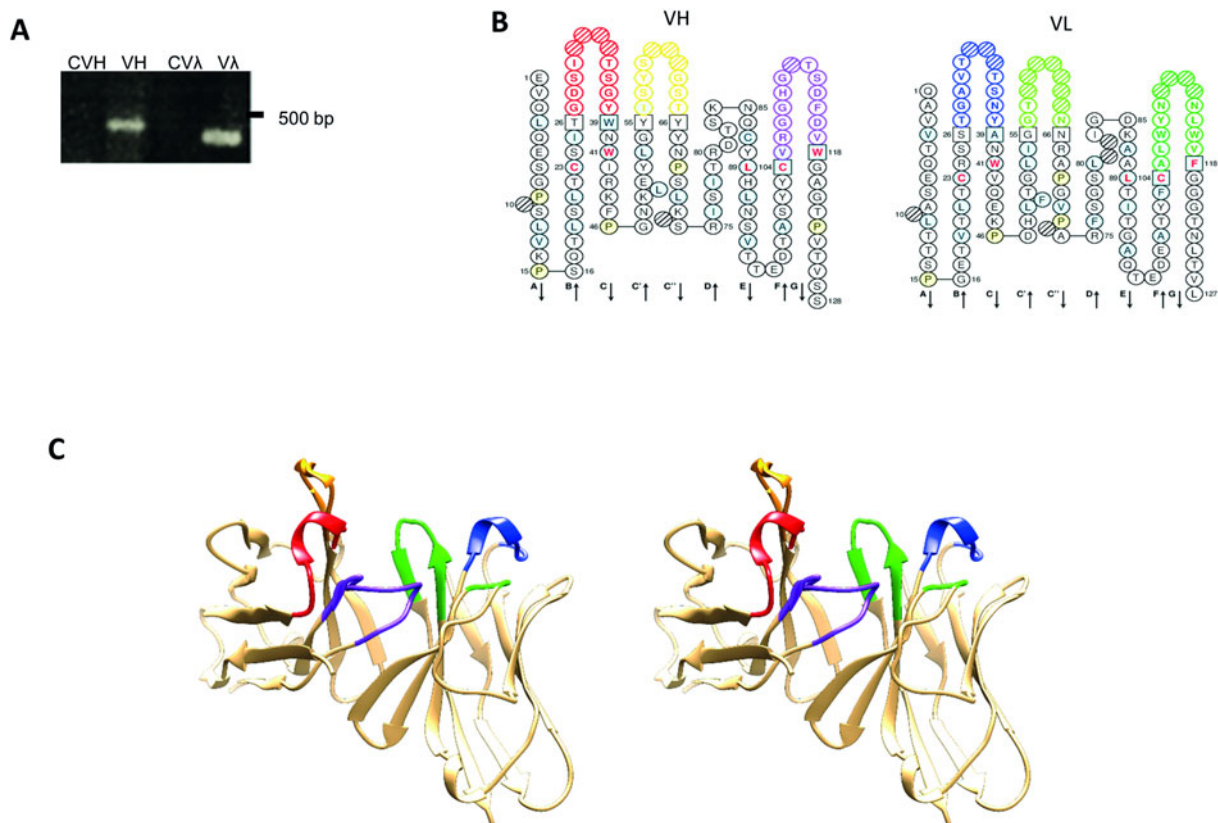


Fig. 1. mAb3V-domains. (A) Agarose gel electrophoresis (1.5%) showing amplification of the antibody's variable heavy chain sequence (VH) with 400 bp and of the lambda light chain sequence (VL) with 350 bp and their respective negative controls (CVH and CVL) without the addition of cDNA. (B) Secondary structure representation of the variable region sequences in the 'collier de perles' analysed by the IMGT and coloured following their colour menu. Heavy (H) and light (L) chain CDRs in red (H1), orange (H2), purple (H3), blue (L1), light green (L2) and forest green (L3); positions in light blue show amino acids with positive values in the hydrophathy index or a tryptophan (W); amino acids shown in red letters correspond to conserved positions of a V-domain; anchor positions are shown in squares; hatched circles indicate gaps according to the unique numbering for V-domains by the IMGT; positions in light yellow show prolines (P); β -strands and their directions indicated by the arrows. (C) Stereo view of three-dimensional structure of the heavy and light variable regions, with coloured CDRs as specified by the IMGT colour menu, the same as previously described.

functional. The VH gene belonged to the IGHV3 murine family and exhibited 96.8% protein sequence identity with *Mus musculus* IGHV3-8*02, whereas the VL gene belonged to the IGLV1 family with 97.9% identity to *M. musculus* IGLV1*01. Figure 1B and C represent the 'collier de perles' and structural model of the mAb3V-domains, respectively.

Mab3 specifically recognizes antigens from pathogenic Acanthamoeba by ELISA and WB assays

The ability of mAb3 to recognize antigens from *Acanthamoeba* strains was demonstrated by ELISA and WB assays. In an indirect ELISA, mAb3 was capable of recognizing only antigens from *Acanthamoeba* strains with pathogenic potential, and in a dose-dependent manner (Fig. 2A). This recognition pattern was also observed by WB as shown in Fig. 2B, in which a band corresponding to the high mass component is recognized in six of the seven samples tested. mAb3 did not recognize components present in the AC-G1 isolate in any of the assays. The capacity of mAb3 to recognize antigens from other agents responsible for causing keratitis was also investigated. No cross-reactivity was detected, proving mAb3 specificity by WB and ELISA (Fig. 2C).

mAb3's target undergoes N-glycosylation and has homology to CPA (Cation: Proton Antiporter) superfamily

Tunicamycin, an N-glycosylation inhibitor, was added to the *Acanthamoeba*'s culture medium to determine if mAb3's target

undergoes N-glycosylation. This was confirmed in a flow cytometry experiment, as shown in Fig. 2D, in which peak displacement suggested a decrease in mAb3 reactivity, probably influenced by disruption of N-glycosylation.

Immunoprecipitation assays with *Acanthamoeba* (AP2) antigens were performed in order to isolate the specific target recognized by mAb3. The eluate sample was analysed by WB, which indicated the isolation of the target protein (Fig. 2E). MS analysis *via de novo* sequencing, based on the most abundant peptides, suggests that the excised sample is homologous to a transporter, a membrane protein part of the CPA2 (Cation: Proton Antiporter2) family. Figure 3 shows the sequence of the supposed mAb3 target and highlights the conserved motif involved in antiporter function, as well as the percentage of identity with other proteins of the CPA2 family.

Flow cytometry and immunofluorescence assays confirmed mAb3's reactivity against pathogenic strains

The reactivity of mAb3 against *Acanthamoeba* trophozoites with pathogenic potential was confirmed by indirect flow cytometry and since no membrane permeabilizer had been used in the cell preparation, it can be assumed that the target is a membrane protein (Fig. 4A1). For all strains with pathogenic potential, significant displacement of the histogram curves was observed when compared to the controls. The specificity for the isolate AR14 was slightly inferior to other strains, but histogram displacement was still evident. The AC-G1 isolate did not interact with mAb3,

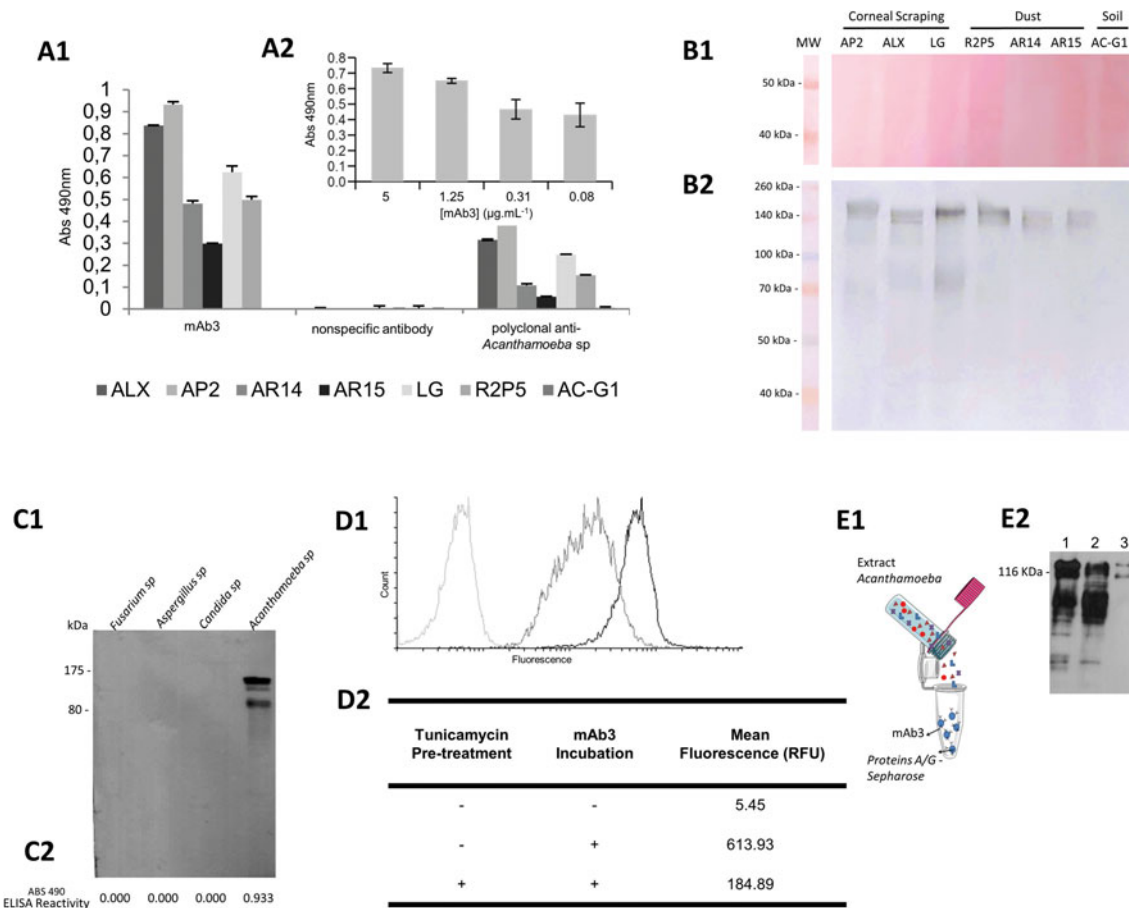


Fig. 2. mAb3 characterization. (A1) Indirect ELISA showing reactivity of mAb3 antibody ($5 \mu\text{g mL}^{-1}$) or irrelevant monoclonal antibody and polyclonal antibodies (1:100) against ALX, AP2, AR14, AR15, LG, R2P5 and AC-G1 *Acanthamoeba* strains sonicated antigens ($10 \mu\text{g mL}^{-1}$), immunocomplexes were revealed using HRP-conjugated anti-mouse IgG (1:4000). (A2) Indirect ELISA showing different concentrations of mAb3 antibody reactivity against strain AP2 ($10 \mu\text{g mL}^{-1}$). (B) WB of AP2, ALX, LG (clinical samples from corneal scrapings of AK patients), R2P5, AR14, AR15 (environmental samples from dust) and AC-G1 (environmental sample from soil) protein extract ($5 \mu\text{g}$) (obtained with lysis buffer) in nitrocellulose membrane stained by Ponceau (B1), followed by incubation with mAb3 ($1.5 \mu\text{g mL}^{-1}$) (B2), immunocomplexes were revealed using HRP-conjugated anti-mouse IgG (1: 10 000) and DAB/chloronaphthol staining. (C) Reactivity of mAb3 against $1.5 \mu\text{g}$ of *Fusarium* sp., *Aspergillus* sp., *Candida* sp. and *Acanthamoeba* sp. sonicated antigens assayed by WB (C1) and indirect ELISA (C2). In WB, proteins were transferred to a PVDF membrane, incubated with $5 \mu\text{g mL}^{-1}$ of mAb3 and HRP-conjugated anti-mouse IgG (1:4000); reaction was revealed by chemiluminescence detection). Indirect ELISA was performed with $10 \mu\text{g mL}^{-1}$ of antigen against $5 \mu\text{g mL}^{-1}$ of mAb3. (D1) Indirect flow cytometry histogram of strain ALX previously treated with tunicamycin incubated with mAb3 (dark grey), untreated ALX incubated with mAb3 (black), untreated ALX without mAb3 (light grey). (D2) Mean fluorescence intensity of events detected by indirect flow cytometry of ALX with (+) or without (-) tunicamycin pre-treatment and mAb3 incubation, quantified in relative fluorescence units (RFU). (E1) Schematic representation of mAb3 immunoprecipitation of target protein. (E2) WB of *Acanthamoeba* sp. sonicated total protein extract ($1.5 \mu\text{g}$) (1); flow through fraction (2) and eluted fraction of immunoprecipitation assay (3). Antigens were transferred to PVDF membrane incubated with mAb3 ($5 \mu\text{g mL}^{-1}$) and HRP-conjugated anti-mouse IgG (1:4000), and the reaction was revealed by chemiluminescence detection.

with consequent overlap with the control curves. Different concentrations (1×10^6 , 1×10^5 , 1×10^4 and 1×10^3) of the ALX strain were evaluated against mAb3 by flow cytometry in order to infer the sensitivity of this technique, and it was possible to detect up to 1×10^4 cells (data not shown).

To verify the capacity of mAb3 to recognize *Acanthamoeba* strains by direct flow cytometry, trophozoites incubated with FITC-conjugated mAb3 (mAb3-FITC) were analysed in the

flow cytometer. The strains AP2, ALX, LG, R2P5, AR14 and AR15 showed higher fluorescence than the negative controls, as evidenced by the displacement of the histogram peaks (Fig. 4A2), and by the statistically significant difference between the mean fluorescence of samples treated with mAb3-FITC when compared to the negative controls (Fig. 4B). Again, mAb3 was unable to recognize the non-pathogenic AC-G1 isolate, as well as observed in the indirect format.

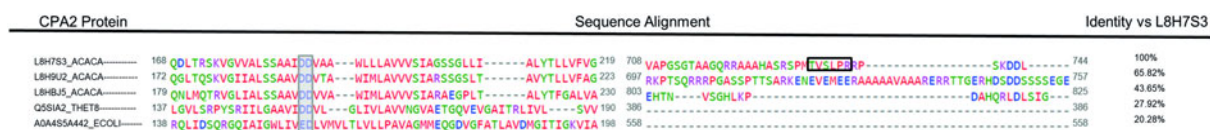


Fig. 3. Multiple amino acid sequence alignment of CPA2 family antiporters, L8HBJ5_ACACA, L8H7S3_ACACA and L8H9U2_ACACA from *Acanthamoeba castellanii*, Q5SIA2_THET8 from *Thermus thermophilus* and A0A4S5A442_ECOLI from *Escherichia coli*. Conserved motif (grey box) involved in antiporter function. The last column shows per cent identity of each sequence when compared to L8H7S3_ACACA, the supposed mAb3 target. Peptide (TVSLPR) found in the mass spectrometry analysis of mAb3's purified target protein (transparent box). Asterisks (*) indicate positions with a fully conserved residue, colons (:) indicate conservation of residues belonging to groups with highly similar properties scoring >0.5 in the Gonnet PAM 250 matrix and periods (.) indicate conservation of residues belonging to groups with weakly similar properties scoring ≤ 0.5 in the Gonnet PAM 250 matrix.

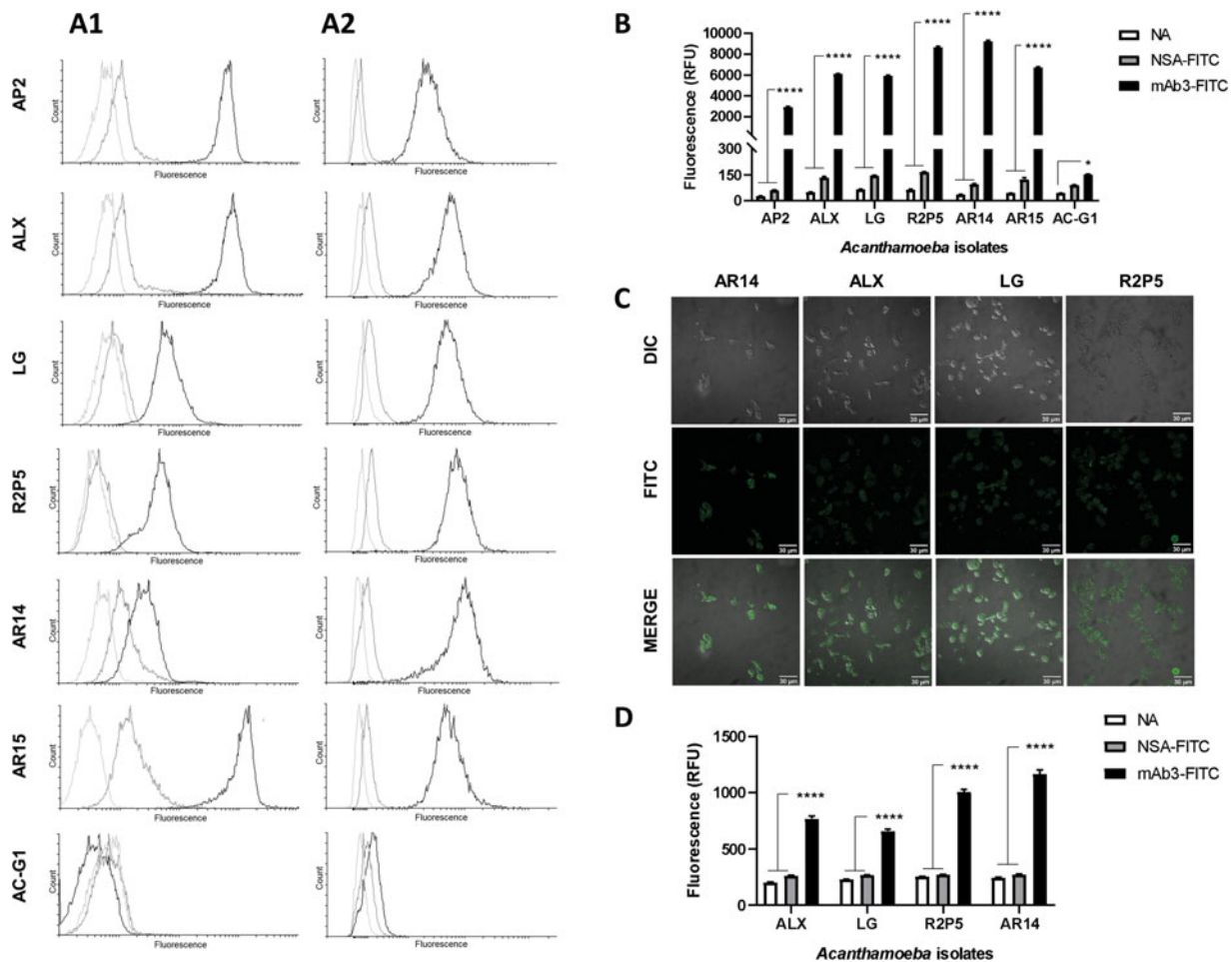


Fig. 4. Reactivity of mAb3 to *Acanthamoeba* strains analysed by flow cytometry and immunofluorescence. (A) Histograms of indirect (A1) and direct (A2) flow cytometry of trophozoites from *Acanthamoeba* strains. Curves in light grey represent samples without antibodies, in dark grey are those treated only with secondary anti-mouse antibody (indirect assay) or FITC-conjugated non-specific IgG (direct assay) and in black are the samples treated with mAb3. (B) Mean fluorescence intensity of events detected by direct flow cytometry of *Acanthamoeba* samples treated with no antibodies (NA), with FITC-conjugated non-specific antibody (NSA-FITC) and with FITC-conjugated mAb3 (mAb3-FITC), quantified in relative fluorescence units (RFU), bars represent mean \pm S.E.M. ($5453 \leq n \leq 10\ 785$), **** $P < 0.0001$, * $P < 0.05$. (C) Direct Immunofluorescence of *Acanthamoeba* trophozoites incubated with FITC-conjugated mAb3, images shown were generated using differential interference contrast (DIC) and fluorescence (FITC) illumination. Autofluorescence of untreated trophozoites was subtracted from the fluorescence intensity observed in the images. (D) Mean fluorescence intensity, detected by direct immunofluorescence, of untreated *Acanthamoeba* trophozoites (NA), treated with FITC-conjugated non-specific antibody (NSA) and with FITC-conjugated mAb3 (mAb3-FITC), quantified in relative fluorescence units (RFU). Bars represent mean \pm S.E.M. ($n = 100$), **** $P < 0.0001$.

To visually evaluate the labeling of *Acanthamoeba* trophozoites by mAb3, strains AR14, ALX, LG and R2P5 were treated with mAb3-FITC and analysed by confocal microscopy. A positive labelling was observed, with fluorescence greater than autofluorescence of untreated cells (Fig. 4C). Absolute fluorescence values were also significantly higher in mAb3-FITC-treated trophozoites than in controls (not treated or treated with non-specific antibody) (Fig. 4D). These results corroborate the findings of flow cytometry.

Mab3 affects early stages of acanthamoeba encystment

Acanthamoeba encystment induced by Neff's medium resulted in a rapid decrease in the percentage of trophozoites in the first 12 h of encystment and consequent increase in the percentage of precysts (PC), followed by transformation of PC in mature cysts, which seems to reach a plateau after 24 h (Fig. 5A).

To evaluate a possible function of the mAb3 target in trophozoites physiological regulation, the kinetics of encystation was verified in the presence of this antibody in the first 12 h of encystment, which seem to be more representative for the main morphological changes in trophozoites. After 8 h, a significant

reduction in the number of trophozoites treated with mAb3 was observed, and the number of precysts increased in the same proportion when compared to the groups treated with vehicle (PBS) or with the nonspecific molecule (Fig. 5B and C). Also, in the first 8 h of encystment, mAb3 induced an increase in precyst formation rate (Fig. 5D), indicating a stimulant effect on encystment in the early steps of the process.

Discussion

The growing number of cases of *Acanthamoeba* infections in recent decades has raised concerns among clinicians, especially due to the limitations of available diagnostic techniques. In the case of GAE, the rarity of the infection makes clinical suspicion difficult and requires expertise for correct identification (Kalra *et al.*, 2020). Delay in specific diagnosis also hampers the management of AK, which can result in many sequelae including irreversible vision loss (Trabelsi *et al.*, 2012). In addition to the methods of direct identification in the affected tissue or culture, nucleic acid amplification has emerged as an alternative for detection with greater sensitivity. However, those molecular techniques are not always available routinely (Dart *et al.*, 2009). Besides, they

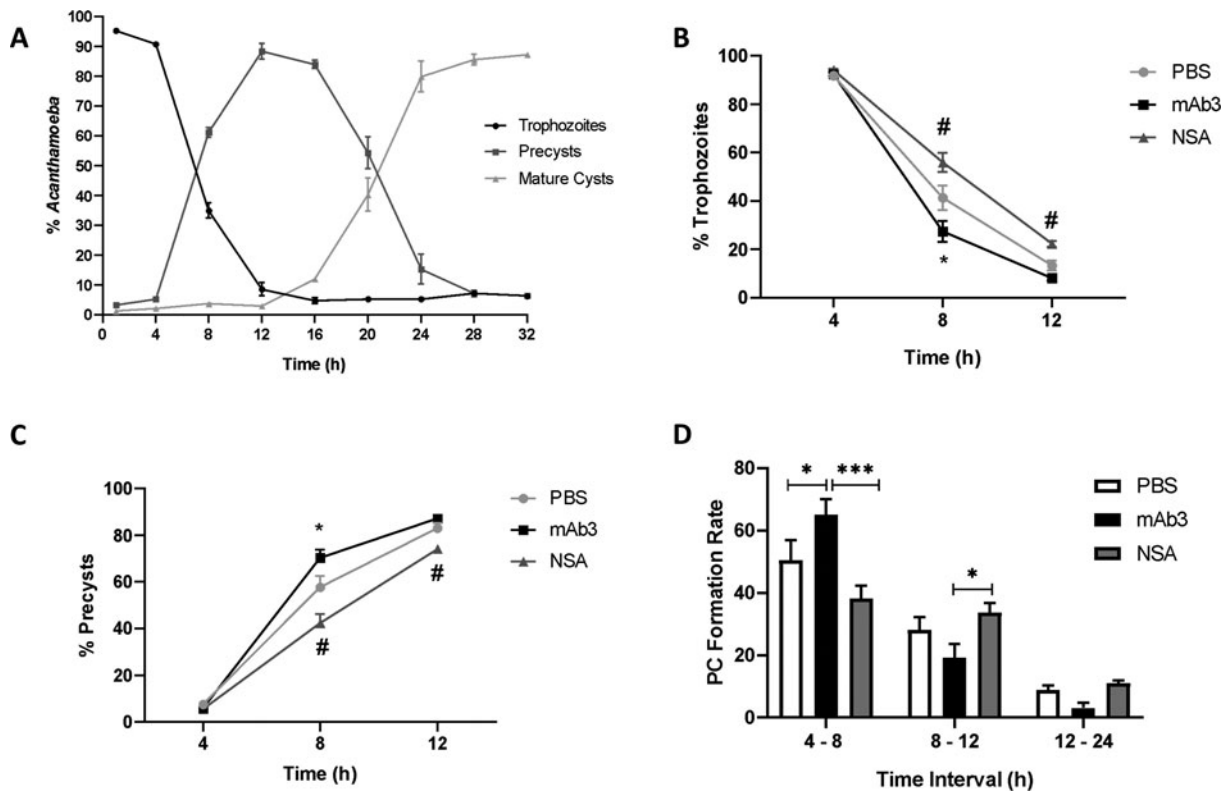


Fig. 5. Effect of mAb3 on *Acanthamoeba* encystation. (A) Kinetics of encystation of *Acanthamoeba* isolate AP2 in Neff's encystation saline, showing the percentage of trophozoites, precyst and mature cysts. (B, C) Effect of mAb3 ($30 \mu\text{g mL}^{-1}$), non-specific antibodies (NSA) ($30 \mu\text{g mL}^{-1}$) and vehicle (PBS) treatment in the amount of trophozoites and precyst. Points in graph represent mean \pm s.e.m. ($n=4$), * $P < 0.01$ mAb3 vs PBS, # $P < 0.01$ mAb3 vs NSA. (D) Effect of mAb3 ($30 \mu\text{g mL}^{-1}$), non-specific antibodies ($30 \mu\text{g mL}^{-1}$) and vehicle (PBS) treatment on precyst (PC) formation rate. Bars represent mean \pm s.e.m. ($n=4$), * $P < 0.05$, *** $P < 0.001$.

can fail in some cases, as reported by Scheid and Balczun (2017), which concluded that the most promising approach is the combination of different diagnostic techniques, including immunological methods.

Monoclonal antibodies are a useful alternative because they identify different pathogens with specificity and can be used in the development of different diagnostic test configurations (Walochnik *et al.*, 2000; Sánchez *et al.*, 2016). The use of polyclonal and monoclonal antibodies in the identification and quantification of parasite antigens in different diagnostic tests is already well known (Andreotti *et al.*, 2003; Ndao, 2009). And over the years, there has been a substitution in the use of polyclonal antibodies by murine and/or recombinant immunoglobulins (Siddiqui, 2010). This is largely because the production of polyclonal antibodies lacks reproducibility and also requires the use of many animals, and thus goes against the guidelines of the 3 Rs (Reduction, Refinement and Replacement). In addition, tests that employ polyclonal antibodies often have issues related to cross-reactivity (Siddiqui, 2010). In this regard, if it is possible to guarantee specificity and sensitivity, the use of monoclonal antibodies is encouraged.

A previous study by Becker-Finco *et al.* (2013) indicated that the monoclonal antibody mAb3 could distinguish pathogenic and nonpathogenic *Acanthamoeba*. We showed presently mAb3's ability to recognize a higher number of strains, all with pathogenic potential corroborating its usefulness in the AK and GAE diagnosis. The analysis of its sequence was important to confirm the monoclonality and its functionality as a murine immunoglobulin, following the recommendations of standardizing the antibodies used in research, having in mind their application in diagnosis (Bradbury and Plückthun, 2015).

MAb3 specificity was confirmed by ELISA, WB, Flow Cytometry and Immunofluorescence and in all tests, the antibody

was able to recognize six of the seven samples tested. Amongst them, ALX, AP2 and LG samples are from clinical origin, being isolated from patients with keratitis (Duarte *et al.*, 2013). AR14 is an environmental isolate (Duarte *et al.*, 2013), and like the previously mentioned strains, also belongs to the T4 genotype, the most frequently associated with infections (Maciver *et al.*, 2013). Another mAb3-reactive strain was AR15, a strain of environmental origin, but belonging to the T11 genotype. T11 is considered the third most abundant genotype in AK (Maciver *et al.*, 2013), which suggests its pathogenic potential. Antigens from the strain R2P5 were also recognized by mAb3, an environmental isolate of T1 genotype (Possamai *et al.*, 2018). This genotype is rare, but it has been associated with cases of GAE, being the second in relevance in this disease (Alsam *et al.*, 2005; Sissons *et al.*, 2006; Maciver *et al.*, 2013). Additionally, this strain presents high protease activity in conditioned medium, a characteristic linked to pathogenicity (Cirelli *et al.*, 2020).

Interestingly, the only *Acanthamoeba* isolate whose proteins were not recognized by mAb3 was AC-G1, a soil-originated sample classified in the morphological group I with no pathogenic effect described until now. However, the AC-G1 isolate does not have the genotype determined so far, but it was characterized as a component from the morphological group I, and would fit into the T7, T8, T9 and T17 genotypes (Magliano *et al.*, 2012), neither of which are associated with infections (Maciver *et al.*, 2013). Conversely, group II *Acanthamoeba* as those recognized by mAb3 presently are more frequent in acanthamoebiasis cases. This suggests that the morphological phenotype can reflect antigenic variation in *Acanthamoeba* lineages.

Additionally, the possibility of cross-reaction with some of the recurrent agents of microbial keratitis was discarded as mAb3 did not recognize antigens from *Fusarium* sp., *Aspergillus* sp. and *Candida* sp. Fungal keratitis can often be misattributed to AK,

leading to delayed treatment and poor prognosis (Walochnik *et al.*, 2000; Mascarenhas *et al.*, 2014).

The use of antibodies to detect *Acanthamoeba* trophozoites by indirect flow cytometry has already been described in the literature (Khan *et al.*, 2000; Turner *et al.*, 2005). All of them were successful, however, the sensitivity and specificity of the analyses were less expressive than those obtained in this work. When mAb3 was conjugated to a fluorophore and used in a direct detection format, the analyses were even more sensitive and still had a shorter runtime.

Concerning mAb3 reactivity, the trophozoites were not permeabilized in the sample preparation and the antibody recognition was still effective, supporting the hypothesis that mAb3's target is a membrane protein, with the region of interaction localized in its extracellular domain (Delmonte and Fleisher, 2019). Furthermore, the findings of the assay with tunicamycin confirmed the importance of carbohydrates at the interaction site. A similar finding was observed by Réveiller *et al.* (2000), who also used tunicamycin to determine whether the target of the monoclonal antibody mAb5D12 anti-*Naegleria fowleri* was influenced by N-glycosylations, showing that the antigenic target had a polysaccharide component.

The confirmation that the mAb3 target is on the cell surface supports the idea of employing it in immunofluorescence tests for detection of *Acanthamoeba* trophozoites. Some laboratories are already using immunofluorescence to aid the diagnosis of AK (Lorenzo-Morales *et al.*, 2015) and several studies utilize this technique to detect trophozoites (Khan *et al.*, 2000; Magnet *et al.*, 2012; Becker-Finco *et al.*, 2013; Kang *et al.*, 2018). However, most of them use polyclonal antibodies and all apply the indirect detection method, which increases the chances of non-specific reactivity and make the protocol more laborious. So far, mAb3's ability to recognize antigens present in trophozoites of the different isolates tested is well established, confirming its potential use in acanthamoebiasis diagnosis. However, diagnostic sensitivity would greatly increase if the antibody was also able to recognize the cystic forms. Preliminary tests were performed and it was possible to observe positive reactivity against several early stages of cyst formation, nonetheless, these findings still need to be confirmed in a larger number of samples.

MS analysis suggested that the mAb3 target protein is a monovalent cation: proton transporter membrane protein (CPA2, antiporter), which belongs to a family of carrier proteins, part of the CPA superfamily. They can be found in bacteria, archaea and eukaryotes (Healy *et al.*, 2014). Among the functionally well-characterized members in this family of transporters are KefB/KefC, efflux proteins in *E. coli* capable of catalysing the K⁺/H⁺ antiport (Healy *et al.*, 2014). These proteins are important for cell survival during exposure to toxic metabolites, possibly because they can release K⁺, allowing H⁺ absorption by modulating the cytoplasmic pH (Fujisawa *et al.*, 2007; Roosild *et al.*, 2010; Healy *et al.*, 2014).

Monovalent cation transport membrane proteins have been also described in *Mycobacterium smegmatis* (Mohan *et al.*, 2015). In single-celled eukaryotes, these proteins were found in *Tetrahymena thermophila* with the function of sodium and potassium ion transport and intracellular pH regulation (Eisen *et al.*, 2006). Recently, Khan's group postulated that ion transporters play a role in sensory perception of surroundings, contributing to regulate *A. castellanii* excystation (Siddiqui *et al.*, 2019). Our findings indicated that mAb3 induced an augment in precyst formation rate in the early stages of encystment, corroborating these proteins as participants in trophozoite differentiation as well.

Additionally, physiological regulatory effects of ion transport proteins in other organisms (Eisen *et al.*, 2006; Fujisawa *et al.*, 2007; Roosild *et al.*, 2010; Healy *et al.*, 2014) could also occur in *Acanthamoeba* as part of an adaptive mechanism to parasitic

living conditions, which would demand greater resistance to oxidative stress caused by host's defense cells. This idea is consistent with the reactivity of mAb3 against strains with pathogenic traits found presently, suggesting that the increased presence of these proteins may be related to the greater potential for pathogenicity.

The greatest challenges concerning amoebic keratitis are finding a fast specific diagnostic method and effective treatment. Some groups are studying *Acanthamoeba* pathophysiology and searching for potential new candidates for pharmaceutical targets (Martín-Navarro *et al.*, 2013, 2014; Lakhundi *et al.*, 2015; Rice *et al.*, 2018; Siddiqui *et al.*, 2019). The findings presented in this study suggest that the monoclonal antibody mAb3 recognizes an extracellular target present only in pathogenic *Acanthamoeba*, demonstrating its potential application in AK diagnosis. In addition, the presence of the antibody seems to alter the dynamics of *Acanthamoeba* encystation. In the future, the confirmation of this effect should be done in greater number of isolates, concomitant to genetic sequence analyses and studies about the expression level of CPA2 family transporters. These proteins are rarely studied in *Acanthamoeba*, but in other microorganisms they seem to play a crucial role in their physiology, supporting the importance of better understanding the role of CPA2 transporters in the context of acanthamoebiasis.

Acknowledgements. We thank CTAF-UFPR for the microscopy images and Mass Spectrometry Platform-PR, Carlos Chagas Institute – Fiocruz for spectrometry analyses. We would also like to thank Dr Breno Beirão, Glaucio Valdameri, Marcel Ramirez and Max Ingberman for their suggestions and kind scientific assistance. We also thank TAXonline – Rede Paranaense de Coleções Biológicas for providing the fungal strains used in this study.

Financial support. This research was supported CAPES (Finance code 001).

Conflicts of interest. The authors state no conflict of interest.

Ethical standards. Not applicable.

References

- Alsam S, Sissons J, Jayasekera S and Khan NA (2005) Extracellular proteases of *Acanthamoeba castellanii* (encephalitis isolate belonging to T1 genotype) contribute to increased permeability in an in vitro model of the human blood-brain barrier. *Journal of Infection* **51**, 150–156.
- Andreotti PE, Ludwig GV, Peruski AH, Tuite JJ, Morse SS and Peruski LF (2003) Immunoassay of infectious agents. *BioTechniques* **35**, 850–859.
- Becker-Finco A, Costa AO, Silva SK, Ramada JS, Furst C, Stingham AE, De Figueiredo BC, De Moura J and Alvarenga LM (2013) Physiological, morphological, and immunochemical parameters used for the characterization of clinical and environmental isolates of *Acanthamoeba*. *Parasitology* **140**, 396–405.
- Bradbury A and Plückthun A (2015) Reproducibility: standardize antibodies used in research. *Nature* **518**, 27–29.
- Bunsuwansakul C, Mahboob T, Houkong K, Laohaprapanon S, Chitapornpan S, Jawjit S, Yasiri A, Barusruks S, Bunluepuech K, Sawangaroen N, Salibay CC, Kaewjai C, de Pereira ML and Nissapatorn V (2019) *Acanthamoeba* in Southeast Asia – overview and challenges. *The Korean Journal of Parasitology* **57**, 341–357.
- Carnt N, Hoffman JJ, Verma S, Hau S, Radford CF, Minassian DC and Dart JKG (2018) *Acanthamoeba* keratitis: confirmation of the UK outbreak and a prospective case-control study identifying contributing risk factors. *British Journal of Ophthalmology* **102**, 1621–1628.
- Chávez-Munigua B, Salazar-Villatoro L, Lagunes-Guillén A, Omaña-Molina M, Espinosa-Cantellano M and Martínez-Palomo A (2013) *Acanthamoeba castellanii* cysts: new ultrastructural findings. *Parasitology Research* **112**, 1125–1130.
- Cirelli C, Mesquita EIS, Chagas IAR, Furst C, Possamai CO, Abrahão JS, dos Santos Silva LK, Grossi MF, Tagliati CA and Costa AO (2020) Extracellular protease profile of *Acanthamoeba* After prolonged axenic culture and after interaction with MDCK cells. *Parasitology Research* **119**, 659–666.

- Da Rocha-Azevedo B and Costa e Silva-Filho F (2007) Biological characterization of a clinical and an environmental isolate of *Acanthamoeba Polyphaga*: analysis of relevant parameters to decode pathogenicity. *Archives of Microbiology* **188**, 441–449.
- Dart JKG, Saw VPJ and Kilvington S (2009) *Acanthamoeba* keratitis: diagnosis and treatment update 2009. *American Journal of Ophthalmology* **148**, 487–499.e2.
- Delmonte OM and Fleisher TA (2019) Flow cytometry: surface markers and beyond. *Journal of Allergy and Clinical Immunology* **143**, 528–537.
- Duarte JL, Furst C, Klisiowicz DR, Klassen G and Costa AO (2013) Morphological, genotypic, and physiological characterization of acanthamoeba isolates from keratitis patients and the domestic environment in Vitoria, Espírito Santo, Brazil. *Experimental Parasitology* **135**, 9–14.
- Duggal S, Rongpharpi S, Duggal A, Kumar A and Biswal I (2017) Role of *Acanthamoeba* in granulomatous encephalitis: a review. *Journal of Infectious Diseases & Immune Therapies* **1**, 1–12.
- Eisen JA, Coyne RS, Wu M, Wu D, Thiagarajan M, Wortman JR, Badger JH, Ren Q, Amedeo P, Jones KM, Tallon LJ, Delcher AL, Salzberg SL, Silva JC, Haas BJ, Majoros WH, Farzad M, Carlton JM, Smith RK Jr, Garg J, Pearlman RE, Karrer KM, Sun L, Manning G, Elde NC, Turkewitz AP, Asai DJ, Wilkes DE, Wang Y, Cai H, Collins K, Stewart BA, Lee SR, Wilamowska K, Weinberg Z, Ruzzo WL, Wloga D, Gaertig J, Frankel J, Tsao CC, Gorovsky MA, Keeling PJ, Waller RE, Patron NJ, Cherry JM, Stover NA, Krieger CJ, del Toro C, Ryder HF, Williamson SC, Barbeau RA, Hamilton EP and Orias E (2006) Macronuclear genome sequence of the ciliate *Tetrahymena thermophila*, a model eukaryote. *PLOS Biology* **4**, 1620–1642.
- Fields C, O'Connell D, Xiao S, Lee GU, Billiard P and Muzard J (2013) Creation of recombinant antigen-binding molecules derived from hybridomas secreting specific antibodies. *Nature Protocols* **8**, 1125–1148.
- Fiori PL, Mattana A, Dessi D, Conti S, Magliani W and Polonelli L (2006) In vitro acanthamoebicidal activity of a killer monoclonal antibody and a synthetic peptide. *Journal of Antimicrobial Chemotherapy* **57**, 891–898.
- Fujisawa M, Ito M and Krulwich TA (2007) Three two-component transporters with channel-like properties have monovalent cation/proton antiport activity. *Proceedings of the National Academy of Sciences* **104**, 13289–13294.
- Healy J, Ekkerman S, Pliotas C, Richard M, Bartlett W, Grayer SC, Morris GM, Miller S and Booth IR (2014) Understanding the structural requirements for activators of the Kef bacterial potassium efflux system. *Biochemistry* **53**, 1982–1992.
- Kalra SK, Sharma P, Shyam K, Tejan N and Ghoshal U (2020) *Acanthamoeba* and its pathogenic role in granulomatous amebic encephalitis. *Experimental Parasitology* **208**, 107788.
- Kang AY, Park AY, Shin HJ, Khan NA, Maciver SK and Jung SY (2018) Production of a monoclonal antibody against a mannose-binding protein of *Acanthamoeba Culbertsoni* and its localization. *Experimental Parasitology* **192**, 19–24.
- Karim-Silva S, Moura JF, Noiray M, Minozzo JC, Aubrey N, Alvarenga LM and Billiard P (2016) Generation of recombinant antibody fragments with toxin-neutralizing potential in loxoscelism. *Immunology Letters* **176**, 90–96.
- Khan NA, Greenman J, Topping KP, Hough VC, Temple GS and Paget TA (2000) Isolation of *Acanthamoeba*-Specific Antibodies from a Bacteriophage Display Library. *Journal of Clinical Microbiology* **38**, 2374–2377.
- Laemmli UK (1970) Cleavage of structural proteins during the assembly of the head of bacteriophage T4. *Nature* **227**, 680–685.
- Lakhundi S, Siddiqui R and Khan N (2015) Cellulose degradation: a therapeutic strategy in the improved treatment of *Acanthamoeba* Infections. *Parasites & Vectors* **8**, 1–16.
- Lorenzo-Morales J, Kliescikova J, Martinez-Carretero E, De Pablos LM, Profotova B, Nohynkova E, Osuna A and Valladares B (2008) Glycogen phosphorylase in *Acanthamoeba* Spp.: determining the role of the enzyme during the encystment process using RNA interference. *Eukaryotic Cell* **7**, 509–517.
- Lorenzo-Morales J, Martín-Navarro CM, López-Arencibia A, Arnalich-Montiel F, Piñero JE and Valladares B (2013) *Acanthamoeba* keratitis: an emerging disease gathering importance worldwide? *Trends in Parasitology* **29**, 181–187.
- Lorenzo-Morales J, Khan NA and Walochnik J (2015) An update on *Acanthamoeba keratitis*: diagnosis, pathogenesis and treatment. *Parasite* **22**, 10.
- Maciver SK, Asif M, Simmen MW and Lorenzo-Morales J (2013) A systematic analysis of *Acanthamoeba* genotype frequency correlated with source and pathogenicity: t4 is confirmed as a pathogen-rich genotype. *European Journal of Protistology* **49**, 217–221.
- Magliano AC, Teixeira MM and Alfieri SC (2012) Revisiting the *Acanthamoeba* species that form star-shaped cysts (genotypes T7, T8, T9, and T17): characterization of seven new Brazilian environmental isolates and phylogenetic inferences. *Parasitology* **139**, 45–52.
- Magnet A, Galván AL, Fenoy S, Izquierdo F, Rueda C, Fernandez Vadillo C, Pérez-Irezábal J, Bandyopadhyay K, Visvesvara GS, da Silva AJ and del Aquila C (2012) Molecular characterization of *Acanthamoeba* Isolated in water treatment plants and comparison with clinical isolates. *Parasitology Research* **111**, 383–392.
- Marciano-Cabral F and Cabral G (2003) *Acanthamoeba* spp. as agents of disease in humans. *Clinical Microbiology Reviews* **16**, 273–307.
- Martín-Navarro CM, Lorenzo-Morales J, Machin RP, López-Arencibia A, García-Castellano JM, de Fuentes I, Loftus B, Maciver SK, Valladares B and Piñero JE (2013) Inhibition of 3-hydroxy-3-methylglutaryl-coenzyme A reductase and application of statins as a novel effective therapeutic approach against *Acanthamoeba* infections. *Antimicrobial Agents and Chemotherapy* **57**, 375–381.
- Martín-Navarro CM, Lorenzo-Morales J, López-Arencibia A, Reyes-Battle M, Piñero JE, Valladares B and Maciver SK (2014) Evaluation of *Acanthamoeba* myosin-1C as a potential therapeutic target. *Antimicrobial Agents and Chemotherapy* **58**, 2150–2155.
- Mascarenhas J, Lalitha P, Prajna NV, Srinivasan M, Das M, D'Silva SS, Oldenburg CE, Borkar DS, Esterberg EJ, Lietman TM and Keenan JD (2014) *Acanthamoeba*, fungal, and bacterial keratitis: a comparison of risk factors and clinical features. *American Journal of Ophthalmology* **157**, 56–62.
- Mohan A, Padiadpu J, Baloni P and Chandra N (2015) Complete genome sequences of a *Mycobacterium smegmatis* laboratory strain (MC2 155) and isoniazid-resistant (4XR1/R2) mutant strains. *Genome Announcements* **3**, e1520–e1514.
- Muinao T, Pal M and Boruah HPD (2018) Cytosolic and transmembrane protein extraction methods of breast and ovarian cancer cells: a comparative study. *Journal of Biomolecular Techniques* **29**, 71–78.
- Ndao M (2009) Diagnosis of parasitic diseases: old and new approaches. *Interdisciplinary Perspectives on Infectious Diseases* **2009**, 1–15.
- Neelam S and Niederkorn JY (2017) Pathobiology and immunobiology of *Acanthamoeba* keratitis: insights from animal models. *The Yale Journal of Biology and Medicine* **90**, 261–268.
- Olli K, Neubert M and Anderson D (2004) Encystment probability and encystment rate: new terms to quantitatively describe formation of resting cysts in planktonic microbial populations. *Marine Ecology Progress Series* **273**, 43–48.
- Pettersen EF, Goddard TD, Huang CC, Couch GS, Greenblatt DM, Meng EC and Ferrin TE (2004) UCSF Chimera? A visualization system for exploratory research and analysis. *Journal of Computational Chemistry* **25**, 1605–1612.
- Possamai CO, Loss AC, Costa AO, Falqueto A and Furst C (2018) *Acanthamoeba* of three morphological groups and distinct genotypes exhibit variable and weakly inter-related physiological properties. *Parasitology Research* **117**, 1995–1995.
- Réveiller L, Marciano-Cabral F, Pernin P, Cabanes PA and Legastelois S (2000) Species specificity of a monoclonal antibody produced to *Naegleria fowleri* and partial characterization of its antigenic determinant. *Parasitology Research* **86**, 634–641.
- Rice CA, Campbell SJ, Bisson C, Owen HJ, Sedelnikova SE, Baker PJ, Rice DW, Henriquez FL and Roberts CW (2018) Structural and functional studies of histidine biosynthesis in *Acanthamoeba* Spp. demonstrates a novel molecular arrangement and target for antimicrobials. *PLoS ONE* **13**, e0198827.
- Roosild TP, Castronovo S, Healy J, Miller S, Pliotas C, Rasmussen T, Bartlett W, Conway SJ and Booth IR (2010) Mechanism of ligand-gated potassium efflux in bacterial pathogens. *Proceedings of the National Academy of Sciences* **107**, 19784–19789.
- Sánchez AGC, Virginio VG, Maschio VJ, Ferreira HB and Rott MB (2016) Evaluation of the immunodiagnostic potential of a recombinant surface protein domain from *Acanthamoeba castellanii*. *Parasitology* **143**, 1656–1664.
- Scheid PL and Balczun C (2017) Failure of molecular diagnostics of a keratitis-inducing *Acanthamoeba* Strain. *Experimental Parasitology* **183**, 236–239.

- Siddiqui M** (2010) Monoclonal antibodies as diagnostics; an appraisal. *Indian Journal of Pharmaceutical Sciences* **72**, 12.
- Siddiqui R, Roberts SK, Ong TYY, Mungroo MR, Anwar A and Khan NA** (2019) Novel insights into the potential role of ion transport in sensory perception in *Acanthamoeba*. *Parasites & Vectors* **12**, 538.
- Sissons J, Alsam S, Goldsworthy G, Lightfoot M, Jarroll EL and Khan NA** (2006) Identification and properties of proteases from an acanthamoeba isolate capable of producing granulomatous encephalitis. *BMC Microbiology* **6**, 42 .
- Szentmáry N, Daas L, Shi L, Laurik KL, Lepper S, Milioti G and Seitz B** (2019) *Acanthamoeba* keratitis – clinical signs, differential diagnosis and treatment. *Journal of Current Ophthalmology* **31**, 16–23.
- Trabelsi H, Dendana F, Sellami A, Sellami H, Cheikhrouhou F, Neji S, Makni F and Ayadi A** (2012) Pathogenic free-living amoebae: epidemiology and clinical review. *Pathologie Biologie* **60**, 399–405.
- Turner ML, Cockerell EJ, Brereton HM, Badenoch PR, Tea M, Coster DJ and Williams KA** (2005) Antigens of selected *Acanthamoeba* species detected with monoclonal antibodies. *International Journal for Parasitology* **35**, 981–990.
- Visvesvara GS, Moura H and Schuster FL** (2007) Pathogenic and opportunistic free-living amoebae: *Acanthamoeba* Spp., *Balamuthia Mandrillar*, *Naegleria fowleri*, and *Sappinia diploidea*. *FEMS Immunology & Medical Microbiology* **50**, 1–26.
- Walochnik J, Haller-Schober E, Kolli H, Picher O, Obwaller A and Aspöck H** (2000) Discrimination between clinically relevant and non relevant *Acanthamoeba* Strains isolated from contact lens-wearing keratitis patients in Austria. *Journal of Clinical Microbiology* **38**, 3932–3936.
- Zhao Z, Worthylake D, LeCour L, Maresh GA and Pincus SH** (2012) Crystal structure and computational modeling of the fab fragment from a protective anti-ricin monoclonal antibody. *PLoS ONE* **7**, e52613.